Ray methods for Free Boundary Problems

J.A.Addison,*
S.D.Howison,†
J.R.King‡

May 25, 2005

Abstract

We discuss the use of the WKB ansatz in a variety of parabolic problems involving a small parameter. We analyse the Stefan problem for small latent heat, the Black–Scholes problem for an American put option, and some nonlinear diffusion equations, in each case constructing an asymptotic solution by the use of ray methods.

1 Introduction

The WKB(J) ansatz, as developed by Green [9] and Liouville [21] among others, is most commonly seen in its application to linear elliptic equations (or to time-harmonic solutions of linear hyperbolic equations) in given domains. Representative examples include Schrödinger's equation when $\hbar$ is considered small (the semiclassical limit) and the Helmholtz equation for large wave numbers, the latter leading to the geometrical theory of diffraction and indeed to the idea of a ray as a characteristic of the leading order approximation, the eikonal equation. In this paper, we describe some cases in which the exponential ansatz typical of the method, and the consequent reduction to a nonlinear first-order equation solved by Charpit's method, can be exploited to construct approximate solutions to some (intrinsically nonlinear) free boundary problems of parabolic and degenerate parabolic type.

In the theory of diffraction, the solution along a given ray typically has the approximate form

$$\text{amplitude} \times \exp(i \times \text{phase}), \tag{1}$$

where the phase, but not the amplitude, varies rapidly along the ray. In our problems, however, the factor i is absent. Instead, the second term in (1) varies rapidly as the exponential of a real quantity; this makes an asymptotic approach

*Mathematical Institute, 24–29 St. Giles', Oxford, OX1 3LB, U.K.
†Mathematical Institute, 24–29 St. Giles', Oxford, OX1 3LB, U.K.
‡Theoretical Mechanics Section, University Park, Nottingham, NG7 2RD,U.K.

especially fruitful. For example, the canonical caustic singularity of diffraction theory does not play a role; instead, the appropriate canonical situation occurs when rays meet on 'ridge lines', where the magnitudes of their contributions to the solution are equal. At other points where two rays cross, one associated solution is typically exponentially smaller in magnitude than the other. A well-known situation in which ridge lines occur is when the height of a sandpile on a table is modelled by the eikonal equation of geometrical optics.

In Section 2 we discuss in some detail the small latent heat limit of the Stefan problem, and a related problem from mathematical finance. In Section 3 we consider more briefly the application of ray methods to degenerate parabolic equations.

2 The Stefan problem with small latent heat

2.1 Formulation

In this section we analyse the small latent heat limit of the Stefan problem for solidification of a pure material. In a general two-phase problem, in which the initial data for the temperature $u(\boldsymbol{x}, t)$ vary by $O(1)$, the phase interface varies only slightly from the $u = 0$ isotherm of the corresponding heat conduction problem and can be found by a regular perturbation scheme. However, if only one phase is active, the other remaining at the phase-change temperature $u = 0$, the behaviour is more subtle.

We therefore consider the following situation: a domain $\Omega \subset \mathbb{R}^n$ is filled with material, initially solid and at the melting temperature, which we shall take to be zero. At time $t = 0$, the temperature on the boundary $\partial\Omega$ is raised to a specified value $g(\boldsymbol{x}, t) > 0$. The solid therefore melts from the boundary inwards, and we wish to describe the evolution of the solid-liquid interface.

Thus, for $t > 0$, $u = 0$ in the solid phase while

$$u_t = \Delta u \tag{2}$$

in the liquid phase, with

$$u = 0, \quad -\frac{\partial u}{\partial n} = \epsilon V_n$$

on the solid-liquid interface $\Gamma(t)$ whose normal velocity (into the solid) is V_n. The initial conditions are

$$u(\boldsymbol{x}, 0) = 0, \quad \Gamma(0) = \partial\Omega.$$

We have chosen units so that the inverse Stefan number

$$\epsilon = (St)^{-1} = \frac{L}{T_0 c} \tag{3}$$

appears in the moving boundary condition rather than the heat equation; here L is the latent heat, k is the thermal conductivity, T_0 is a typical temperature scale and c is the specific heat.

We are interested in the limit $\epsilon \to 0$, the case of 'weak' or 'slight' nonlinearity. (In the opposite limit when ϵ is large, it is necessary to scale so that the coefficient in the moving boundary conditions is 1, and the heat equation $\Delta u = \epsilon u_t$ is thus approximated by $\Delta u = 0$. This 'extremely' nonlinear limit is known as the Hele-Shaw problem; we include some instances of this case too, for comparison.) When $\epsilon = 0$, the phase-change is instantaneous. We thus anticipate that for $\epsilon \ll 1$ and $g(\boldsymbol{x}, t)$ not everywhere small, melting occurs on a much shorter timescale than that implicit in the scalings above, a result which is also clear from a consideration of the energy required to melt the solid, $\epsilon|\Omega(0)|$ in dimensionless units, compared with the flux in from the boundary. The correct scalings are, however, not immediately obvious, and it is easiest to derive them first from a particular one-dimensional solution.

2.2 The Neumann solution to the one-dimensional problem

2.2.1 The explicit solution

In one spatial dimension, say for $\Omega = (0, \infty)$ with the applied temperature at $x = 0$, the phase change interface can be written as $x = s(t; \epsilon)$ and the Stefan problem above simplifies to

$$u_t = u_{xx}, \quad 0 < x < s(t; \epsilon), \tag{4}$$

$$u(x, 0) = 0, \quad s(0; \epsilon) = 0, \tag{5}$$

$$u(0, t) = g(t), \tag{6}$$

and at $x = s(t; \epsilon)$

$$u = 0, \quad u_x = -\epsilon \dot{s}. \tag{7}$$

When $g(t) = g_0 =$ constant, there is a similarity solution, the 'Neumann' solution (due to Lamé and Clapeyron [20]):

$$u(x, t) = g_0 \left(1 - \int_0^{x/t^{1/2}} e^{-\eta^2/4} d\eta \Big/ \int_0^{\alpha} e^{-\eta^2/4} d\eta \right), \tag{8}$$

$$s(t; \epsilon) = \alpha(\epsilon) t^{1/2}, \tag{9}$$

where $\alpha(\epsilon)$ is determined from the transcendental equation

$$\frac{\epsilon \alpha e^{\alpha^2/4}}{2} \int_0^{\alpha} e^{-\eta^2/4} d\eta = g_0. \tag{10}$$

It is then easy to show from (10) that as $\epsilon \to 0$,

$$s(t; \epsilon) \sim 2(t/\delta)^{1/2},$$

where

$$\delta = 1/|\log \epsilon|.$$

This suggests that in order to analyse $O(1)$ changes in $s(t;\epsilon)$, we must rescale time with δ:

$$t = \delta T. \tag{11}$$

It is now straightforward to show that the solution has an asymptotic structure consisting of three regions. The first is a boundary layer near the fixed boundary $x = 0$, in which $x = O(\delta^{1/2})$; in this layer the solution is to leading order the zero-latent heat solution. In the second region x is of $O(1)$, and this region matches into the third region, an interior layer of width $O(\delta)$ near the interface $x = s(t;\epsilon)$ in which the solution is to leading order a travelling wave. We now give further details of the three regions and their matching; of course they can easily be shown to be consistent with the exact solution (8). It is known rigorously that the result for the limiting behaviour of $s(t;\epsilon)$ is correct for this and more general one-dimensional problems. This follows from [22]; the analysis there is however confined to one spatial dimension.

2.2.2 The boundary layer near $x = 0$

We recall that in (11) we rescaled time by δ. In order to achieve a balance in the heat equation we set

$$x = \delta^{1/2} X,$$

and, with $u = u_0(X,T) + o(1)$ as $\epsilon, \delta \to 0$, the solution satisfying $u(0,T) = g_0$ is

$$u_0 = g_0 \mathrm{erfc}(X/2T^{1/2});$$

we shall comment on more general boundary conditions later. As $X \to \infty$, this solution has the asymptotic behaviour

$$u_0 \sim \frac{2g_0 T^{1/2}}{\pi^{1/2} X} e^{-X^2/4T}, \tag{12}$$

and this must match into the second region.

2.2.3 The 'outer' region $x = O(1)$

In this region, x is unscaled and so we must solve

$$\delta^{-1} u_T = u_{xx}, \tag{13}$$

with $u(x,0) = 0$. As $x \to 0$, the solution must match with (12). Written in outer variables, (12) is

$$u_0 \sim \frac{2g_0 T^{1/2} \delta^{1/2}}{\pi^{1/2} x} e^{-x^2/4\delta T},$$

and this suggests the ansatz

$$u \sim \delta^{1/2}(a_0(x,T) + \ldots)e^{-f(x,T)/\delta}. \tag{14}$$

Note also that the exponential term in (14) may be thought of as a WKB ansatz for (13). Substitution into (13) yields

$$f_T = -f_x^2, \tag{15}$$

$$a_{0T} = -2f_x a_{0x} - f_{xx}a_0. \tag{16}$$

The characteristic projections of (15) (obtained by Charpit's method) are $x/T =$ constant, so f and a_0 are determined by matching back into the boundary layer (which can be viewed as a canonical 'diffraction' problem) for small x, T with $x/T = O(1)$, giving

$$f \sim x^2/4T \quad \text{and} \quad a_0 \sim 2g_0 T^{1/2}/\pi^{1/2}x \quad \text{as} \quad x, T \to 0.$$

In this case, the solution is identical to its limiting form, namely

$$f = x^2/4T, \quad a_0 = 2g_0 T^{1/2}/\pi^{1/2}x. \tag{17}$$

We must now match this solution into the neighbourhood of the phase change interface.

2.2.4 The interior layer near the free boundary

Near the free boundary, we expect the solution to be, to leading order, a travelling wave. Recalling that $ds/dt = O(\delta^{-1})$, when we change to coordinates moving with the free boundary the dominant contribution to the left-hand side of (13) is of $O(\delta^{-2})$. It is therefore appropriate to write

$$x = s(t;\epsilon) + \delta\xi = S(T;\delta) + \delta\xi,$$

and, in order to achieve a balance in the latent heat condition,

$$u = \epsilon U.$$

The leading order problem is

$$-(dS_0/dT)U_{0\xi} = U_{0\xi\xi},$$

and, imposing the moving boundary conditions $U_0 = 0, U_{0\xi} = -dS_0/dT$, we have

$$U_0 = e^{-\xi dS_0/dT} - 1. \tag{18}$$

This must match with (14); using (17) we write (14) in inner variables as

$$u \sim \left(\frac{2g_0\delta^{1/2}T^{1/2}}{\pi^{1/2}S} + \cdots\right)e^{-S^2/4\delta T - \xi S_0/2T + \cdots}. \tag{19}$$

Recalling also that $u = \epsilon U = e^{-1/\delta}U$, matching (18) with (14) requires

$$S \sim 2T^{1/2}(1 - \delta(\log\delta - \log(\pi/g_0))/4), \tag{20}$$

completing our reconstruction of the Neumann solution for small ϵ and. indeed, providing a more accurate approximation to $s(t;\epsilon)$ than that given earlier.

2.3 One-dimensional problems: discussion

2.3.1 More general one-dimensional problems

It is easy to generalise the results above to the case where the prescribed temperature at $x = 0$ is not constant, and hence there is no similarity solution. It can be seen that the constant g_0 does not affect the leading order behaviour of $s(t;\epsilon)$, since this entirely controlled by the exponential factor in (4), which does not depend on g_0. It therefore follows from (20) that to leading order

$$s(t;\epsilon) \sim 2|\log\epsilon|^{-1/2}t^{1/2}, \tag{21}$$

for any boundary data $u(x,0) = g(t)$ for which g_0 is neither exponentially small nor large in δ, and for which $g(t)$ does not vary by $O(1)$ on any timescale faster than $O(\delta)$. Because the interior layer is small, it also follows that the location of the free-boundary is to leading order the isotherm $U = \epsilon$ of the corresponding heat conduction problem *without* solidification. A further consequence is that if we consider, for example, solidification of the interval $0 < x < 1$, with $u(0,t) = g(t), u(1,t) = h(t)$, we have the rather surprising result that the two interfaces meet, to leading order, at the mid-point $x = 1/2$ at dimensionless time $\delta/4$. This result, in fact, holds even if g and h vary by $O(1)$ on the timescale $T = O(1)$.

A further generalisation is provided by an example which illustrates the difference between the 'extremely' and 'slightly' nonlinear limits in which the inverse Stefan number is respectively large and small (see Section 2.1 above, and Section 3). We consider (4)–(6) with $g(t) = t^\alpha, \alpha > -1$. If $\alpha \neq 0$, so that the Neumann solution does not apply, we can rescale to set $\epsilon = 1$ in (6). The two limiting cases are then as follows.

(i) 'Large' inverse Stefan number.

If the left-hand side of (4) is negligible, $u(x,t)$ is linear in x. We have

$$u \sim t^\alpha f(x/t^{(\alpha+1)/2}), \quad f(\eta) = 1 - ((\alpha+1)/2)^{1/2}\eta, \tag{22}$$

with

$$s \sim (2/(\alpha+1))^{1/2}t^{(\alpha+1)/2}.$$

If $\alpha > 0$, (22) represents a consistent balance in (4) as $t \to 0^+$ and thus gives the small-time behaviour. Conversely, if $-1 < \alpha < 0$ it provides the large-time behaviour.

(ii) 'Small' inverse Stefan number.

Following the approach outlined in Section 2, the boundary layer solution is the zero Stefan number similarity solution

$$u \sim t^\alpha f(x/t^{1/2}),$$

with

$$\begin{aligned} &\alpha f - \eta f_\eta/2 = f_{\eta\eta}, \\ &f = 1 \quad \text{at} \quad \eta = 0, \\ &f \sim A\eta^{-(2\alpha+1)} e^{-\eta^2/4} \quad \text{as} \quad \eta \to \infty, \end{aligned} \tag{23}$$

where the value of the positive constant A can be determined by solving (23), which can be done in terms of parabolic cylinder functions. Matching into the interior layer, the free boundary location can then be shown to satisfy

$$s^2 \sim 4t(\alpha \log t - (\alpha + 1/2)\log(4\alpha \log t) + \log A). \tag{24}$$

As is clear from the sign of the leading term in (24), the limit required for these results to apply is $t \to \infty$ for $\alpha > 0$ and $t \to 0^+$ for $-1 < \alpha < 0$.

In order to describe the asymptotic behaviour completely, both limit cases must thus be analysed. For $-1 < \alpha < 0$, (22) provides the large-time behaviour and (24) the small-time; the reverse is true for $\alpha > 0$. As is well-known, in the borderline case $\alpha = 0$ the solution is, as described in §2.2, exactly self-similar and depends rather sensitively on the value of the Stefan number. In the other cases the effective Stefan number varies with time in a manner made apparent by the above analysis.

2.3.2 The Grinberg and Chekmareva approach

An alternative approach to the one-dimensional case is to use the Laplace transform to reformulate the Stefan problem as a nonlinear integral equation for $s(t;\epsilon)$. This approach follows the idea of [10], also used by [6] and [22] (with a prescribed heat flux at $x = 0$). We take the Laplace transforms of (4)–(7), defining the Laplace transform of $u(x,t)$ by

$$\bar{u}(x,p) = \int_{\omega(x)}^{\infty} u(x,t) e^{-pt} dt,$$

where $\omega(x) \equiv s^{-1}(x)$ is well-defined if we assume that $g(t) \geq 0$, since then $s(t)$ is increasing. A short calculation shows that

$$\bar{u}_{xx} - p\bar{u} = \epsilon e^{-p\omega(x)}, \qquad x \geq 0, \quad \Re(p) > 0, \tag{25}$$

with

$$\bar{u}(0,p) = \bar{g}(p) \quad \text{and} \quad \bar{u} \to 0 \quad \text{as} \quad x \to \infty.$$

Solving (25), inverting with the aid of the convolution theorem, and returning to $s(t)$ as the dependent variable, we find the integral equation

$$\begin{aligned} s(t) \int_0^t g(t-\tau) e^{-s(t)^2/4\tau} \frac{d\tau}{\tau^{3/2}} = \\ \epsilon \int_0^t \dot{s}(t-\tau) \big(e^{-(s(t)-s(t-\tau))^2/4\tau} - e^{-(s(t)+s(t-\tau))^2/4\tau} \big) \frac{d\tau}{\tau^{1/2}}. \end{aligned}$$

We can then obtain the leading order behaviour of $s(t;\epsilon)$ by substituting in the ansatz $s(t;\epsilon) \sim \alpha(\epsilon)t^{1/2}$ as above, and confirm the results of Section 2.2. Note, however, that although this approach readily gives details of $s(t;\epsilon)$, it is less helpful concerning the structure of $u(x,t)$; nor is it useful in more than one space dimension.

2.4 The American put option

The method described above leads to a quick derivation of the asymptotic behaviour of the Black–Scholes value of an American put option near its expiration date; moreover, unlike certain other approaches (see [3, 8, 17, 18] for related studies) it can readily be generalised, for example to higher dimensions (see [4] for a different approach in more than one dimension). We recall (see [25]) that in this model the value of such an option satisfies a backwards parabolic equation with terminal (payoff) values given at the expiration time $t = T$. It is convenient to measure time backwards from this expiration date, so we write $t' = T - t$. Let us consider an American put option, namely an option to sell an asset with price S for a strike price K at any (physical) time up to expiration, that is for $t' \geq 0$, and write its value as $V(S,t')$. The payoff value is $\max(K-S,0)$ and the terminal ($t' = 0$) value of the option is

$$V(S,0) = \max(K-S,0), \quad 0 < S < \infty.$$

The option value satisfies the parabolic (time-reversed Black–Scholes) equation

$$V_{t'} = \frac{1}{2}\sigma^2 S^2 V_{SS} + (r-q)SV_S - rV \tag{26}$$

for $S^*(t') < S < \infty$; here σ is the volatility of the asset price returns, r the risk-free rate and q the continuous dividend yield. Also $S^*(t')$ is the optimal exercise boundary, at which

$$V = K - S, \quad V_S = -1;$$

these conditions state that the option value is equal to the payoff at $S = S^*(t')$, and the Delta, V_S, is continuous there. For $S < S^*(t')$ we have $V = K - S$. The case $r > q$ is of most financial interest as this is usually the case in practice, and then the free boundary emanates from $S = K$ and moves to the left. (If $r < q$, the free boundary emanates from $S = rK/q$ with square-root-in-time behaviour as in the corresponding problem for an American call option [25], into which it can be transformed. This case can arise for FX options but is unusual for stock or equity index options. If $r = q = 0$ there is no free boundary.)

We now adopt the rescalings

$$S = K\hat{S}, \quad S^* = K\hat{S}^*, \quad V = K\hat{V}, \quad t' = 2\hat{t}/\sigma^2$$

to give, dropping the hats,

$$\frac{\partial V}{\partial t} = S^2\frac{\partial^2 V}{\partial S^2} + \rho(1-\theta)S\frac{\partial V}{\partial S} - \rho V,$$

with

$$V(S,0) = \max(1-S,0), \qquad S^*(0^+) = \min(1,1/\theta),$$

the free boundary conditions

$$V(S^*(t),t) = 1 - S^*(t), \quad \frac{\partial V}{\partial S} = -1,$$

and, lastly, $V \to 0$ as $S \to \infty$; here $\rho = 2r/\sigma^2$, $\theta = q/r$. The case of financial interest is that in which $0 \le q < r$, so that $0 \le \theta < 1$, and this is the only case we consider. Our final reformulation expresses the problem in the manner most reminiscent of the Baiocchi-transformed version of the Stefan problem (i.e. the oxygen-consumption problem) by subtracting the payoff from V and discounting, and changing to moving log-price coordinates, setting

$$V = 1 - S + e^{-\rho t}\Psi(\zeta,t), \quad \zeta = \log S - (1-\rho(1-\theta))\,t,$$

which yields

$$\frac{\partial \Psi}{\partial t} = \frac{\partial^2 \Psi}{\partial \zeta^2} + \rho\theta e^{\zeta} e^{(1+\rho\theta)t} - \rho e^{\rho t}, \tag{27}$$

with

$$\Psi(\zeta,0) = \max(e^{\zeta}-1,0), \quad \zeta^*(0^+) = \min(0,-\log\theta),$$

the free boundary conditions

$$\Psi = \frac{\partial \Psi}{\partial \zeta} = 0 \tag{28}$$

on $\zeta = \zeta^*(t)$, and $\Psi \sim e^{\zeta}e^{(1+\rho\theta)t} - \rho e^{\rho t}$ as $\zeta \to \infty$; here $\zeta^*(t) = \log S^*(t) - (1-\rho(1-\theta))\,t$. It is worth noting that the 'latent heat' term in (28), namely $e^{\zeta}e^{(1+\rho\theta)t} - \rho e^{\rho t}$, is negative for sufficiently large ζ but positive for $\zeta < -(1-\rho(1-\theta)t) - \log\theta$ (i.e. for $S < 1/\theta$), the former corresponding to an ill-posed Stefan problem and the latter to a well-posed one; the interplay between the two has important consequences for the dynamics, and the moving boundary is always located in the latter regime. In particular, the instantaneous jump in the free boundary to $S^*(0^+) = 1/\theta$ when $\theta > 1$ can be interpreted similarly to a comparable situation for the Stefan problem described in [11]. Although we do not consider further the case $\theta > 1$, as indicated above such a jump occurs for an American call option when $0 < \theta < 1$ [25].

The problem is amenable to ray methods not only in the limit of small time, but also for small 'latent heat', $\rho \to 0$. We focus on the latter; it corresponds to a small interest-rate regime and would be especially appropriate in markets such as Japan in the early years of the 21st century, where annualised interest rates were less than 1% (0.01), whereas in the same units for an individual stock σ might be as much as 0.4, so that $\rho \approx 0.125$. While related results have been obtained elsewhere (see [17], in particular), it seems appropriate to revisit the problem in the context of the rather general framework developed here. For brevity, our presentation of the asymptotics will be slightly informal, but we stress that they can be made fully systematic.

Our starting point is the corresponding European Put solution

$$\Psi_E(\zeta,t)=\frac{1}{2}\left(\mathrm{erfc}(\zeta/2t^{1/2})-e^{\zeta+t}\mathrm{erfc}\left((\zeta+2t)/2t^{1/2}\right)\right)+e^{\zeta+(1+\rho\theta)t}-e^{\rho t}. \tag{29}$$

This is the solution to (27) with the same initial condition but with the conditions on $\zeta=\zeta^*(t)$ replaced by

$$\Psi_E\sim 1-e^{\rho t}+e^{\zeta}\left(e^{(1+\rho\theta)t}-e^{t}\right)$$

as $\zeta\to-\infty$. That is, it is the solution with no constraint and it plays a role similar to that which the heat-conduction solution plays in the Stefan problem above. Indeed, while (29) contains our small parameter ρ, it serves as an outer solution which is uniformly valid across the relevant timescales. A key result we require from (29) is the more detailed far-field expression

$$\Psi_E\sim 1-e^{\rho t}+e^{\zeta}\left(e^{(1+\rho\theta)t}-e^{t}\right)+\frac{2t^{3/2}}{\pi^{1/2}\zeta(\zeta+2t)}e^{-\zeta^2/4t} \tag{30}$$

as $\zeta\to-\infty$ with $t=O(|\zeta|)$ and $\zeta/t<-2$; the final term in this expression is of the expected form

$$t^{-1/2}A(\zeta/t)e^{-\zeta^2/4t},$$

with the 'directivity' $A(\sigma)$ given in this case by

$$A(\sigma)=\frac{2}{\pi^{1/2}\sigma(\sigma+2)}.$$

Setting $\zeta=\zeta^*(t)+\xi$, when ρ is small a putative leading-order inner balance (whose range of validity can be checked *a posteriori* in the usual way) reads

$$-\dot\zeta^*\frac{\partial\Psi}{\partial\xi}\sim\frac{\partial^2\Psi}{\partial\xi^2}-\rho\left(1-\theta e^{\zeta^*+t}\right) \tag{31}$$

so that

$$\Psi\sim\frac{\rho}{\dot\zeta^{*2}}\left(1-\theta e^{\zeta^*+t}\right)\left(e^{-\dot\zeta^*\xi}-1+\dot\zeta^*\xi\right). \tag{32}$$

Matching the exponential in ξ from (32) with the corresponding exponential from the final term of (30) as $\xi\to+\infty$ (recall that $\zeta^*<0$, $\dot\zeta^*<0$), shows that, for $0\le\theta<1$,

$$\dot\zeta^*\sim\frac{\zeta^*}{2t}$$

and hence, matching the amplitudes of the exponential terms, that (since $\zeta^*(t)\gg t$ here)

$$\frac{1}{2(\pi t)^{1/2}}e^{-\zeta^{*2}/4t}\sim\rho\left(1-\theta e^{\zeta^*+t}\right). \tag{33}$$

For $t=O(1)$ we have $-\zeta^*\gg1$, so the θ terms in (31)–(33) are in fact negligible. and hence

$$\zeta^{*2}\sim-2t\log(4\pi\rho^2t); \tag{34}$$

the appropriate scalings in (32) for $t = O(1)$ are thus $\xi = O(1/|\log\rho|^{1/2})$, $\Psi = O(\rho/|\log\rho|)$. For $\theta = 0$, no earlier timescales are needed; when $\theta > 0$, however, a distinct early-time balance occurs in (33) for

$$t = \bar{t}/|\log\rho|, \quad \zeta^* = -2\bar{t}^{1/2}\left(1 + \frac{\log|\log\rho|}{4|\log\rho|} + \frac{\bar{z}^*(\bar{t})}{|\log\rho|}\right),$$

whereby the θ terms cannot be neglected and the dominant balance in (33) becomes

$$\bar{z}^* \sim -\frac{1}{4}\log\left(4\pi\bar{t}\left(1 - \theta e^{-2\bar{t}^{1/2}}\right)^2\right). \tag{35}$$

Returning to the regime $t = O(1)$, from (34) we have

$$\zeta^* \sim -2t^{1/2}|\log\rho|^{1/2} + \frac{1}{2}t^{1/2}\frac{\log(4\pi t)}{|\log\rho|^{1/2}} \tag{36}$$

for $t = O(1)$. The families of rays associated with the final term in (30) and with the term $e^{\zeta+t}$ are given respectively by $\zeta/t =$ constant and $\zeta + 2t =$ constant, and we might anticipate that (36) will cease to be valid for $t \sim |\log\rho|$, when $\zeta = \zeta^*(t)$ lies on the coincident ray $\zeta/t = -2$. However, the balances above in fact first change subtly on the intermediate timescale $t = |\log\rho|T$, where $0 < T < 1$, and $\zeta^* = |\log\rho|Z^*$. This follows because (33) is then replaced by

$$\frac{2T^{3/2}}{\pi^{1/2}Z^*\,(Z^* + 2T)\,|\log\rho|^{1/2}}e^{-Z^{*2}|\log\rho|/4T} \sim \frac{\rho}{\dot{Z}^{*2}}, \tag{37}$$

so that

$$Z^* \sim -2T^{1/2} + \frac{\log|\log\rho|}{2|\log\rho|}T^{1/2} + \frac{1}{|\log\rho|}T^{1/2}\log\left(2(\pi T)^{1/2}(1 - T^{1/2})\right), \tag{38}$$

providing further evidence that a change in behaviour is to be expected at $T = 1$.

The next timescale, then, has scalings

$$t = |\log\rho| + |\log\rho|^{1/2}\tau, \quad \zeta^* = -2|\log\rho| - |\log\rho|^{1/2}\tau + z^*(\tau) \tag{39}$$

and, for the inner region,

$$\zeta = -2|\log\rho| - |\log\rho|^{1/2}\tau + z,$$

whereby, in view of (29), which is equivalent to

$$\Psi_E(\zeta,t) = \tfrac{1}{2}\left(e^{\zeta+t}\mathrm{erfc}\left(-(\zeta+2t)/2t^{1/2}\right) - \mathrm{erfc}\left(-\zeta/2t^{1/2}\right)\right) + e^{\zeta+t}\left(e^{\rho\theta t} - 1\right) - \left(e^{\rho t} - 1\right),$$

we find that (30) is replaced when $\tau = O(1)$ by

$$\Psi \sim \frac{1}{2}\rho e^z\mathrm{erfc}(-\tau/2) \tag{40}$$

as the matching condition on the inner region as $z \to +\infty$ for $\rho \ll 1$.

The dominant balance for $z = O(1)$ is

$$\frac{\partial \Psi}{\partial z} \sim \frac{\partial^2 \Psi}{\partial z^2} - \rho \tag{41}$$

with

$$\Psi = \frac{\partial \Psi}{\partial z} = 0$$

at $z = z^*$, so that

$$\Psi \sim \rho \left(e^{z - z^*} - 1 - (z - z^*) \right).$$

Thus, on matching with (40) we obtain

$$z^* \sim -\log\left(\operatorname{erfc}(-\tau/2)/2\right). \tag{42}$$

Before outlining the final timescales, we note that the large-time behaviour is given asymptotically by the steady state solution

$$V_\infty(S) = \frac{1}{\nu + 1} \left(\frac{(\nu + 1)S}{\nu} \right)^{-\nu}, \qquad S^*(\infty) = \frac{\nu}{\nu + 1},$$

where ν, the negative of the relevant root of the indicial equation for the time-independent scaled Black–Scholes equation, is given by

$$\nu = -\frac{1}{2} \left((1 - \rho(1 - \theta)) - \left((1 - \rho(1 - \theta))^2 + 4\rho \right)^{1/2} \right) = \rho + O(\rho^2) \quad \text{as } \rho \to 0.$$

This corresponds to a travelling wave solution for $\Psi(\zeta, t)$ having

$$\zeta^*(t) \sim -|\log \rho| - t \quad \text{as } \rho \to 0$$

with which (39), (42) are already consistent as $\tau \to \infty$. In order to complete the asymptotic description of the solution, we must now nevertheless describe the further regime $T > 1$, for which the relevant matching condition between inner and outer regions becomes

$$\Psi_E \sim 1 - e^{\rho t} + e^{\zeta + (1 + \rho\theta)t} + \frac{2t^{3/2}}{\pi^{1/2} \zeta(\zeta + 2t)} e^{-\zeta^2/4t} \tag{43}$$

as $\zeta \to -\infty$ with $t = O(|\zeta|)$, $\zeta/t > -2$. This condition replaces (30) (one of the terms in (30) no longer appears, because the location $\zeta = -2t$ at which the relevant Stokes lines are born has passed beyond the moving boundary). It is then the third, rather than the last, term of (32) that appears on matching for $T > 1$, i.e. (37) is replaced by

$$e^{|\log \rho|(Z^* + T)} \sim \frac{\rho}{\dot{Z}^{*2}},$$

from which we recover

$$Z^* \sim -1 - T. \tag{44}$$

In view of (27) in particular, the final timescale is naturally seen be $t = t^\dagger/\rho$, and the change of variables

$$\zeta = -t^\dagger/\rho - |\log \rho| + \zeta^\dagger$$

is needed to resolve the inner region, in which the analysis is now more delicate. We have

$$\rho \frac{\partial \Psi}{\partial t} + \frac{\partial \Psi}{\partial \zeta^\dagger} = \frac{\partial^2 \Psi}{\partial {\zeta^\dagger}^2} - \rho e^{t^\dagger} + \rho^2 \theta e^{\zeta^\dagger + \theta t^\dagger}, \tag{45}$$

so the matching condition derived from (43), namely

$$\Psi \sim \rho e^{\zeta^\dagger + \theta t^\dagger}$$

as $\zeta^\dagger \to +\infty$, on the leading-order inner solution (whereby $\Psi = O(\rho)$) requires that

$$\frac{\partial \Psi}{\partial \zeta^\dagger} \sim \rho \left(e^{\zeta^\dagger + \theta t^\dagger} - e^{t^\dagger} \right).$$

The interface accordingly satisfies

$$\zeta^\dagger \sim (1-\theta) t^\dagger \tag{46}$$

as required. Finally, by setting

$$\zeta^\dagger = (1-\theta) t^\dagger + \rho^{-1/2} \xi^\dagger, \quad \Psi = e^{\frac{1}{2}\rho^{-1/2}(1-\rho(1-\theta))\xi^\dagger - \frac{1}{4}\rho^{-1}(1-\rho(1-\theta))^2 t^\dagger} \Phi(\xi^\dagger, t^\dagger)$$

in the homogeneous version of (45), we recover the heat equation, whose dipole solution governs how $S^*(t)$ approaches the steady state, involving an algebraic modulation to the exponential rate $e^{-\frac{1}{4}\rho^{-1}(1-\rho(1-\theta))^2 t^\dagger}$; this also applies for $\rho = O(1)$.

In summary, we have obtained explicit expressions for ζ^* in each of the asymptotic regimes, namely (35) on the shortest timescale $\bar{t} = O(1)$ (in fact, an additional subtlety arises for even shorter times, but this is captured by the small-time solution (47) noted below), (36) for $t = O(1)$, (38) for $T = O(1)$ with $T < 1$, (39) and (42) on the transition timescale $\tau = O(1)$, (44) for $T = O(1)$ with $T > 1$, and finally (46) for $t^\dagger = O(1)$. The ray interpretation of the results (with the two distinct families of rays carrying the crucial matching information from (29)) is indispensable in motivating the various asymptotic scenarios and confirming their self-consistency.

Finally we consider the local analysis of the free boundary near expiration. This has been treated in [18, 8, 17, 3] via an integral equation approach. This behaviour can also readily be analysed within our framework, and indeed a minor modification of (34) applies, namely

$$\zeta^2 \sim -2t \log \left(4\pi \rho^2 (1-\theta)^2 t \right) \tag{47}$$

as $t \to 0$ for $\rho = O(1)$, by essentially the same arguments as those above (cf. (33)). We stress that our approach generalises immediately to higher-dimensional problems, again as shown in the following section.

2.5 Higher-dimensional problems

2.5.1 Matched asymptotic expansions approach

The methods of Section 2.2 generalise easily to the case where Ω is a bounded domain in $\mathbb{R}^n$, initially filled with solid at the melting temperature. Now there is a melted region $L(t)$, bounded by $\partial\Omega$ and by the phase change interface $\Gamma(t)$. The model we adopt for $t > 0$ is equations (2)–(3) with

$$u = g(\boldsymbol{x}, T) \qquad \boldsymbol{x} \in \partial\Omega,$$

where g satisfies the conditions detailed in Section 2.3.1. Again, time is scaled with $\delta = 1/|\log \epsilon|$ and there is a three-layer structure.

2.5.2 Boundary layer near $\partial\Omega$

The solution here is as in Section 2.2.2; X is now given by $X = x_n/\delta$, where x_n represents distance into $L(t)$ normal to $\partial\Omega$. Note that if $\partial\Omega$ is not smooth this approximation may not be uniformly valid (consider, for example, melting the interior or exterior of a corner in two dimensions). We shall return to this point below.

2.5.3 Outer Region

In the 'outer' region, in which distances from $\partial\Omega$ are $O(1)$, we generalise (14) to

$$u \sim \delta^{1/2}(a_0(\boldsymbol{x}, T) + \ldots)e^{-f(\boldsymbol{x},T)/\delta}. \tag{48}$$

We only calculate $f(\boldsymbol{x}, T)$ here; this is sufficient to determine the leading order position of the free boundary. As we saw in Section 2.2.2, $a_0(x, T)$ only contributes to a small correction to this leading order behaviour, and for the same reason the leading order behaviour of $\Gamma(T)$ is independent of the boundary data $g(\boldsymbol{x}, T)$, provided that the latter is neither too large nor too small nor varies too rapidly. We find that

$$f_T = -|\boldsymbol{\nabla} f|^2, \tag{49}$$

with $f \sim x_n^2/4T$ as x_n, the distance to $\partial\Omega$, tends to zero with x_n/T remaining $O(1)$. The solution of (49) takes the separable form

$$f(\boldsymbol{x}, T) = \big(F(\boldsymbol{x})\big)^2/4T,$$

from which we recover the eikonal equation of geometrical optics,

$$|\boldsymbol{\nabla} F|^2 = 1,$$

with $F = 0$ on $\partial\Omega$. The solution is just

$$F = x_n,$$

so

$$f(\boldsymbol{x}, T) = x_n^2/4T.$$

This solution is valid sufficiently close to $\partial\Omega$ that the characteristic projections, which are the normals to $\partial\Omega$, do not cross, and may again require qualification if $\partial\Omega$ is not smooth.

2.5.4 Interior layer near $\Gamma(T)$

The solution in the interior layer is as before, ξ now representing distance along the normal to $\Gamma(T)$. Matching with the outer region requires simply that the leading order location of the moving boundary is determined by where $f = 1$, i.e.

$$x_n = 2T^{1/2}.$$

This is evidently consistent with (20).

2.6 Discussion

We can summarise the results above by saying that, to leading order, the phase change interface advances along the normals to $\partial\Omega$ with speed $(\delta t)^{-1/2}$, independently of the boundary data (provided the latter is uniformly neither large nor small). We return to the case of variable boundary data below. Thus, the last point to melt is that furthest from $\partial\Omega$. As in the one-dimensional case, the location of $\Gamma(t)$ is to leading order the isotherm $U = \epsilon$ of the corresponding pure heat conduction problem; as before, the solution in the boundary and outer regions is not to leading order influenced by the inner layer near $\Gamma(t)$, and the superlinearity in the exponential term in the outer layer determines the location of Γ quite precisely. This scenario may require some modifications, for example when the characteristic projections (normal to $\partial\Omega$) cross, or when $\partial\Omega$ is not smooth.

Even if $\partial\Omega$ is smooth, the characteristic projections must eventually meet. (For an analysis of the late stages of the special case of melting a sphere (but with large Stefan number), see [23, 24].) When they do cross, the dominant contribution is from those on which the distance to $\partial\Omega$ is shortest. The leading order moving boundary determined by our procedure may then not be smooth, and the inner region is no longer one-dimensional. For example, if $\partial\Omega$ is an ellipse, the leading order approximation to $\Gamma(t)$ first becomes irregular at the foci, with $X \sim \text{const.}|Y|^{4/3}$ in local variables (X, Y). For later times, the leading order approximation to $\Gamma(t)$ has two finite-angle corners which move in from the foci towards the centre of the ellipse (see Figure 1). If on the other hand $\partial\Omega$ is a square and Ω its interior, 'ridge-line' discontinuities are present for all $t > 0$ along the diagonals: $\Gamma(t)$ is to leading order a square, distance $2(t/\delta)^{1/2}$ inwards normally from $\partial\Omega$, but our approximation is clearly invalid at its corners. In such cases, an inner travelling-wave free boundary problem is easily formulated to describe the smoothing of the outer solution [16].

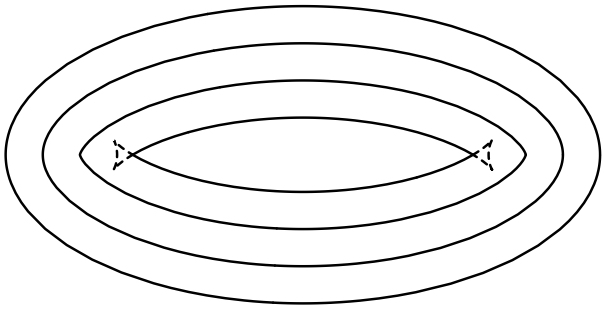

Figure 1: Melting of the interior of an ellipse. The outer ellipse is $\partial\Omega$; moving inwards, $\Gamma(t)$ is shown before it becomes irregular at the foci, at the moment it becomes irregular and at a later time. Only the solid portion of the innermost curve contributes to $\Gamma(t)$; on the dashed portion, the relevant ray carries an exponentially subdominant amplitude.

Lastly if $\partial\Omega$ has reentrant corners, for example, the leading order approximation to $\Gamma(t)$ consists of smooth segments constructed from the normals to the smooth parts of $\partial\Omega$, joined up by 'expansion fans' emanating from the corners. Thus, for example, if Ω is the exterior of a square of side a, the approximation to $\Gamma(t)$ consists of straight line segments (normal translations of the sides through a distance $2(t/\delta)^{1/2}$) joined by arcs of circles centred on the corners. Both reentrant and non-reentrant corners occur in models for options on several assets.

3 Nonlinear diffusion

3.1 Preamble

We now illustrate the more widespread applicability of ray methods to moving boundary problems by noting two generalisations of the Hamilton-Jacobi formulation of the limit problem $m \to 0^+$ of

$$u_t = \boldsymbol{\nabla} \cdot (u^m \boldsymbol{\nabla} u), \tag{50}$$

which has been exploited by [12].

We firstly consider more general nonlinearities, i.e. we treat

$$u_t = \boldsymbol{\nabla} \cdot (D(u) \boldsymbol{\nabla} u), \tag{51}$$

where $D(u)$ depends on some small positive parameter ϵ; we shall give a general form of this dependence for which ray methods are applicable in the limit $\epsilon \to 0$.

As with (50), the key step is a change of dependent variable. It is instructive to consider two such transformations, the second of which gives the formulation appropriate to the application of ray methods; the first is not relevant to such approaches, being included for comparison.

The change of variable $w = D(u)$.

The change of variable $w = D(u)$ transforms (51) into

$$w_t = w\Delta w + \big(D(u)/D'(u)\big)'|\boldsymbol{\nabla} w|^2. \tag{52}$$

If $D(u)$ is such that the third term is negligible in (50), we have

$$w_t = w\Delta w. \tag{53}$$

The circumstances under which this occurs (the simplest of which is $m \to \infty$, as for example in [7]) are discussed in [13]. This represents the 'extremely nonlinear' limit of (51), a limiting case analogous to the Hele-Shaw limit of the Stefan problem (see Sections 2.1 and 2.3.1). A particular feature worth noting is that separable solutions $w = W(\boldsymbol{x})/t$ satisfy the linear problem

$$\Delta W = -1,$$

the 'squeeze-film' variant of the Hele-Shaw problem (see [19]).

The change of variable $v = \int_0^u D(u')du'/u'$.

In this case we have

$$v_t = |\boldsymbol{\nabla} v|^2 + D\Delta v; \tag{54}$$

when the third term is negligible, which is the case of interest here (we give examples below), we have

$$v_t = |\boldsymbol{\nabla} v|^2. \tag{55}$$

This represents the 'slightly nonlinear' limit of (51). As we saw earlier, it also arises on applying the WKB method to the heat equation (see (49)), and thus complements (53).

3.2 Solutions with moving boundaries

Many nonlinear diffusion problems have solutions with moving boundaries. We consider two generalisations of the WKB method to analyse such problems, beginning with the equations considered in the previous section.

The requirement that the interface $u = 0$ of (51) exhibit finite speed of propagation is that the integral $\int_0^u D(u')du'/u'$ be bounded; that is the case we

treat here. For any suitable $D(u)$, both (54) and its approximation (55) have the exact travelling wave solution

$$v = q(qt - x)_+, \tag{56}$$

and this more generally describes the local behaviour at an interface moving with speed q.

We therefore now illustrate the circumstances under which (54) can be approximated by (55) by taking

$$D(u;\epsilon) = \epsilon\psi(\epsilon \log u), \quad \psi(0) = 1, \quad \psi(-\infty) = 0, \tag{57}$$

for example $D(u;\epsilon) = \epsilon u^\epsilon$. For definiteness we consider the Cauchy problem with compactly supported initial conditions of the form

$$v = V(\boldsymbol{x}) \quad \text{at} \quad t = 0,$$

where $V(\boldsymbol{x})$ is independent of ϵ and has its global maximum at $\boldsymbol{x} = \boldsymbol{0}$. We normalise the problem such that $V(\boldsymbol{0}) = \Psi(0)$, where $\Psi(\sigma) = \int_{-\infty}^{\sigma} \psi(\sigma')d\sigma'$; this is bounded for finite propagation speed. From (57) we thus have

$$v = \Psi(\epsilon \log u), \quad D(u) = \epsilon/\Phi'(v),$$

where $\Psi(\Phi(v)) = 1$, implying

$$u = \exp(\Phi(v)/\epsilon), \tag{58}$$

which is the appropriate WKB ansatz here. In the outer region $|\boldsymbol{x}| = O(1)$, with $v \sim v_0(\boldsymbol{x}, t)$ as $\epsilon \to 0$, we have the ray problem

$$\begin{aligned} v_{0_t} &= |\boldsymbol{\nabla} v_0|^2, \\ v_0 &= V(\boldsymbol{x}) \quad \text{at} \quad t = 0, \end{aligned} \tag{59}$$

from which the leading order moving boundary location for $t = O(1)$ can be determined from where $v_0 = 0$. We note that the solution v_0 to (59) is decreasing along characteristics, so that (59) in fact holds only where $v_0 > 0$; elsewhere $v_0 = 0$ applies.

There is also an inner region $\boldsymbol{x} = \epsilon^{1/2}\boldsymbol{X}$. Choosing axes such that

$$V(\boldsymbol{x}) \sim \Phi(0) - \sum_{i=1}^{N} \alpha_i x_i^2 \quad \text{as} \quad |\boldsymbol{x}| \to 0,$$

for positive constants α_i, then the leading order inner solution $u \sim u_0(\boldsymbol{X}, t)$ satisfies

$$\begin{aligned} u_{0_t} &= \Delta u_0, \\ u_0 &= \exp\left(- \sum_{i=1}^{N} a_i X_i^2 \right) \quad \text{at} \quad t = 0, \end{aligned}$$

where $a_i = \alpha_i/\Phi'(0)$, so that [14]

$$u_0 = \exp\Big(-\sum_{i=1}^{N} a_i X_i^2/(1+4a_i t)\Big)\Big/\prod_{i=1}^{N}(1+4a_i t)^{1/2}.$$

Simple examples in which the approach applies include

$$D(u) = \epsilon u^{\epsilon} = \epsilon v,$$

and

$$D(u) = \epsilon(1-\epsilon\log u)^{-n} = \epsilon\big((n-1)v\big)^{n/(n-1)} \quad \text{for} \quad n > 1.$$

We now turn to our second generalisation, which concerns the doubly nonlinear equation (see [1] for related considerations)

$$u_t = \boldsymbol{\nabla}\cdot(u^m|\boldsymbol{\nabla}u|^{n-1}\boldsymbol{\nabla}u), \tag{60}$$

with $n > 0$. It is instructive first to note the instantaneous source solution (cf. [2])

$$u = t^{-N/((m+n-1)N+n+1)} f(r/t^{1/((m+n-1)N+n+1)}),$$

with

$$\begin{aligned} f^{(m+n-1)/n} &= \frac{(m+n-1)(a^{(n+1)/n} - \eta^{(n+1)/n})_+}{(n+1)((m+n-1)N+n+1)^{1/n}}, \quad m+n>1,\\ f &= a\exp\big(-n\big(\eta/(n+1)\big)^{(n+1)/n}\big), \qquad\qquad m+n=1,\\ f^{-(1-m-n)/n} &= \frac{(1-m-n)(a^{(n+1)/n} + \eta^{(n+1)/n})_+}{(n+1)(n+1-(1-m-n)N)^{1/n}},\\ &\qquad m+n<1 \text{ with } N<(n+1)/(1-m-n), \end{aligned}$$

for some constant a. The solution is thus compactly supported for $m+n>1$ only; the case we discuss here corresponds to the limit $m+n\to 1^+$. We define

$$v = \frac{n}{m+n-1}u^{(m+n-1)/n},$$

to give

$$v_t = |\boldsymbol{\nabla}v|^{n+1} + \frac{m+n-1}{n}v\boldsymbol{\nabla}\cdot(|\boldsymbol{\nabla}v|^{n-1}\boldsymbol{\nabla}v). \tag{61}$$

The limit problem for $m+n\to 1^+$ is thus

$$v_t = |\boldsymbol{\nabla}v|^{n+1}. \tag{62}$$

Where $v>0$, (62) provides the leading order solution to (60) where u is exponentially small and, in particular, determines the location of the moving boundary,

on which $u = 0$. For given initial data $v = V(\boldsymbol{x})$ at $t = 0$, equation (62) is straightforward to solve via Charpit's equations, with the usual considerations applying when characteristic projections intersect, and we shall not elaborate further here.

Our remaining comments largely concern the limit case $n = 0$, which is a singular limit of (60); we do not give a detailed discussion, merely noting that in the one-dimensional case (60) then reduces to

$$\frac{\partial u}{\partial x}\left(\frac{\partial u}{\partial t} - \frac{\partial}{\partial x}\left(u^m \mathrm{sgn}\left(\frac{\partial u}{\partial x}\right)\right)\right) = 0,$$

and is readily solved. For example, taking $m = 1$ and initial conditions $u = U(x)$ at $t = 0$ with $U'(x)$ negative for x positive (and vice versa) then we have

$$\begin{aligned} u &= U(x - t) \qquad \text{for} \quad x < s_-(t), \\ u &= M(t) \qquad \text{for} \quad s_-(t) < x < s_+(t), \\ u &= U(x + t) \qquad \text{for} \quad x > s_+(t), \end{aligned}$$

where $M(t) = U(s_- + t) = U(s_+ - t)$ is determined by conservation of mass. The solution thus contains additional moving boundaries $s_\pm(t)$.

For $n = 0$, (62) becomes

$$v_t = |\boldsymbol{\nabla} v|, \tag{63}$$

which implies that the outward normal velocity of any level set of v is unity. Thus different level sets, and in particular the moving boundary $v = 0$, can be tracked separately. This is not true for other values of n; only for $n = 0$ is v constant along characteristics of (62), its exceptional status in this regard being consonant with its role as a singular limit. However, the required solution to (62) for $n > 0$ is commonly of the form

$$v = 1 - \frac{n}{t^{1/n}}\left(\frac{F(\boldsymbol{x})}{n+1}\right)^{(n+1)/n},$$

so that

$$|\boldsymbol{\nabla} F| = 1. \tag{64}$$

Writing the moving boundary (or indeed any level set) of (63) as $t = F(\boldsymbol{x})$ we again obtain (64). Under such circumstances the same formulation is appropriate for any $n \geq 0$, the moving boundary being given by

$$F(\boldsymbol{x}) = (n+1)t^{1/(n+1)}/n^{n/(n+1)}.$$

4 Conclusion

We have shown that the WKB ansatz provides an effective approximation for a wide variety of parabolic free-boundary problems in which the evolution of the

free boundary is rapid, facilitating their asymptotic solution explicitly by ray methods. We considered the one-phase Stefan problem in some detail, showing that the location of the phase-change interface is to leading order that of the $U = \epsilon$ isotherm of the corresponding pure conduction problem. To leading order, the interface (isotherm) propagates with constant speed in directions normal to $\partial\Omega$; the last point to melt is the furthest point from the boundary. This point is also the instantaneous minimum, at $t = 0^+$, of the corresponding conduction problem. Subject to certain constraints, these results do not depend on the precise behaviour of the applied boundary temperature. We also discussed more briefly several nonlinear diffusion problems in which a similar asymptotic approach can successfully be employed, illustrating the broad applicability of the technique to extensive classes of moving boundary problems. The outcome is that we can both extract the behaviour of limiting cases and derive analytically tractable reduced problems that can be used to provide insight that is instructive beyond such limiting regimes. It is particularly striking that the approach readily provides results in any number of dimensions, a feature that may be particularly valuable in the context of mathematical finance where the large number of assets involved can cause very severe computational difficulties. Our final remark (cf. [15]) is that the approach is also well suited to certain problems in mathematical biology in which degradative enzymes occur which are so well suited to their specific roles that models of their action lead to what is in effect the small Stefan number regime described above.

Acknowledgements

JRK and JAA gratefully acknowledge financial support from EPSRC.

References

[1] Aronson, D.G., Gil, O. & Vazquez, J.–L. (1998). Limit behavior of focusing solutions to nonlinear diffusions. *Comm. P.D.E.* **23** 307–332.

[2] Barenblatt, G.I. (1952) On self-similar motions of a compressible fluid in a porous medium. *P.M.M.* **16** 419–436.

[3] Chen, X., & Chadam, J. (2004). A mathematical analysis for the optimal exercise boundary of an American put option. *Preprint*.

[4] Chevalier, E. (2004), Free boundary near the maturity of an American option on several assets. *Working paper*.

[5] Crank, J. (1984) *Free and Moving Boundary Problems.* Oxford University Press.

[6] Dewynne, J.N., Howison, S.D., Ockendon, J.R. & Xie, W. (1989) Asymptotic behaviour of solutions to the stefan problem with a kinetic condition at the free boundary. *J. Austral. Math. Soc. Ser. B* **31** 81–96.

[7] Elliott, C.M., Herrero, M.A., King, J.R. & Ockendon, J.R. (1986) The mesa problem: diffusion patterns for $u_t = \boldsymbol{\nabla} \cdot (u^m \boldsymbol{\nabla} u)$ as $m \to +\infty$. *IMA J. Appl. Math.* **37** 147–154.

[8] Evans, J.D., Keller, J.B & Kuske, R. (2002) American options with dividends near expiry. *Mathematical Finance* **12** 219–237.

[9] Green, G. (1837) On the motion of waves in a variable canal of small depth and width. *Trans. Camb. Phil. Soc.* **6**

[10] Grinberg, G.A. & Chekmareva, O.M. (1971) Motion of phase interface in Stefan problems. *Sov. Phys. Tech. Phys.* **15** 1579–1583.

[11] Gurtin, M.E. (1994) Thermodynamics and the supercritical Stefan equations with nucleation. *Q. Appl. Math.* **52**, 133–155.

[12] Kath, W.L. & Cohen, D.S. (1982) Waiting-time behaviour in a nonlinear diffusion equation. *Stud. Appl. Math.* **67** 79–105.

[13] King, J.R. (1993) Multidimensional singular diffusion. *J. Eng. Math.* **27** 357–387.

[14] King, J.R. (1993) Exact multidimensional solutions to some nonlinear diffusion equations. *Q.J.M.A.M.* **46** 419–436.

[15] King, J.R., Koerber, A.J., Croft, J.M., Ward, J.P., Williams, P. & Sockett, R.E. (2003). Modelling host tissue degradation by extracellular bacterial pathogens. *Math. Med. Biol.* **20**, 227–260.

[16] King, J.R., Riley, D.S. & Wallman, A.M. (1999) Two-dimensional solidification in a corner. *Proc. R. Soc. Lond.* **A455** 3449–3470.

[17] Knessl, C. (2002). Asymptotic analysis of the American call option with dividends. *Europ. J. Appl. Math.* **13** 587–616.

[18] Kuske, R. & Keller, J.B. (1998). Optimal exercise boundary for an American put option. *Applied Mathematical Finance* **5** 107–116.

[19] Lacey, A.A. & Ockendon, J.R. (1985) Ill-posed free boundary problems. *Control and Cybernetics* **14** 275–296.

[20] Lamé, G. & Clapeyron, B.P. (1831) Mémoir sur la solidification par refroidissement d'un globe liquide. *Ann. Chem. Phys.* **47** 250–256.

[21] Liouville, J. (1837) Sur le développement des fonctions ou parties de fonctions en séries. *J. Math. Pures Appl.* **2** (1837) 16–35.

[22] Sherman, B. (1971) Limiting behavior in some Stefan problems as the latent heat goes to zero. *SIAM J. Appl. Math.* **20** 319–327.

[23] Soward, A.M. (1980) A unified approach to Stefan's problem for spheres and cylinders. *Proc. R. Soc. Lond.* **A373** 131–147.

[24] Stewartson, K. & Waechter, T.T. (1976) On Stefan's problem for spheres. *Proc. R. Soc. Lond.* **A348** 415–426.

[25] Wilmott, P., Howison, S.D. & Dewynne, J.N. (1995). *The Mathematics of Financial Derivatives*. Cambridge University Press.